European Journal of Molecular & Clinical Medicine
ISSN 2515-8260 Volume 07, Issue 07, 2020

A Two-Dimensional Model To Estimate The Effect Of Calcium Diffusion In Circular Shape Hepatocyte

Vijendra Singh Rawat[1], Rinku Mathur [2],

[1]Department of Mathematics, Teerthanker Mahaveer University, U. P., India
[2] Department of Mathematics, School of Chemical Engineering & Physical Sciences, Lovely Professional University, Phagwara, Jalandhar, India

[1] vijendra.engineering@tmu.ac.in , [2] rinkumathur56@gmail.com

Abstract: Hepatocyte is the primary functional cell of the liver. More than 80 % of liver is constructed by the hepatocyte cell. Calcium is working as a second messenger. The particular cytosolic Ca^{2+} level in hepatocyte cell is responsible for frequently working of the liver. In signal transduction calcium play an essential role in hepatocyte cell. Many biological processes are controlled by the calcium like secretion, muscular contraction, cell differentiation, movement of cell, signaling in cell and processes of buffering etc. Diffusion of calcium in the cell is represented by the reaction-diffusion equations. Here two-dimensional model is developed to estimate the effect of the essential biophysical parameters as association coefficient, bound buffer, influx and coefficient of diffusion over profiles of calcium on hepatocyte cell. The aim of the study is to analyze the effect of cytosolic calcium diffusion in hepatocyte cell when the buffer is present in large amount. The results have been used to establish the relationships among various biophysical parameters.

Keywords: Reaction Diffusion, Hepatocyte cell, Calcium, Buffer, FEM.

1. Introduction

Calcium dynamics govern an essential role to start and completion of all the processes in every cell as hepatocytes, astrocytes, lymphocyte, cardiomyocyte and oocytes etc. As we already know that cytosolic calcium makes a chain of signals and works as a second messenger in every cell. Cytosolic calcium signaling has been used in signal transduction, and changes the electrical signal into the chemical signal [1,5]. Many crucial physiological processes like flow of bile, bile glycogen breakdown, secretion of bile and cell survival in liver is controlled by Cytosolic calcium [2]. Calcium signals can be elicited in isolated cells by a large array of stimuli and often occurs as repetitive calcium waves [3]. Lot of theoretical work has been done to elaborate the mechanism underlying calcium profile oscillations and the phenomenon of calcium waves spreading across multiple connected cells [4]. The free cytosolic calcium concentration ($[Ca^{2+}]$) oscillations elicited by a given agonist concentration differs between individual hepatocytes [5, 6]. In non-excitable cell, self-sustained calcium oscillations were first observed in 1980s [7].

2. Problem Formulation

The reaction diffusion equations are used to simulate the change in concentration of buffer in intracellular calcium profile in the hepatocyte cell. Near isolated point sources the buffered diffusion of Ca^{2+} can be represented by a system of equations [2,5].

$$C + P_i \underset{k^-}{\overset{k^+}{\Longleftrightarrow}} CP_i \tag{1}$$

Where C is the calcium profile, P_i represents free buffer, k^+ association rate constants, k^- dissociation rate constants and CP_i represent bound buffer, for i^{th} species of buffer. Here we consider the reaction of calcium and buffer obeys mass action kinetics. The coupled equation for each species the change in concentration can be written as -

$$\frac{\partial[\mathrm{C}]}{\partial t} = D_C \nabla^2[\mathrm{C}] + \sum_i R_i + \sum F \tag{2}$$

$$\frac{\partial[P_i]}{\partial t} = D_{P_i} \nabla^2[P_i] + R_i \tag{3}$$

$$\frac{\partial[CP_i]}{\partial t} = D_{CP_i} - R_i \tag{4}$$

$$R = -k_i^+[C][P_i] + k_i^-[CP_i] \tag{5}$$

where R and F are common reaction terms and calcium flux respectively.

In absence of influx for steady state condition equation (2) will be-

$$\frac{\partial[C]}{\partial t} = D_C \nabla^2[C] - \sum_i K_i^+[P_i]_\infty([C]-[C]_\infty) \tag{6}$$

In the presence of excess buffering approximation (EBA), a numerical approach (FEM) has to be developed for the diffusion process of calcium in cell. In this model the various crucial parameters as dissociation rate constant, amplitude of source, diffusion rate, and rate of binding are incorporates. Taking the polar cylindrical coordinates in equation (6) can be written as

$$D_C\left(\frac{1}{r}\frac{\partial}{\partial r}\left(r\frac{\partial}{\partial r}\right)+\frac{1}{r}\frac{\partial}{\partial \psi}\left(\frac{1}{r}\frac{\partial}{\partial \psi}\right)\right)[C]-K_n^+[P]_\infty([C]-[C]_\infty)+\sigma\,\delta(r)=0 \tag{7}$$

In the above equation $[P]_\infty$ and $[C]_\infty$ are the concentration of buffer and concentration of calcium respectively. Here consider the circular shape hepatocytes cell and divided into forty eight circular elements. The number in circle and without circle denotes the elements and the nodal points respectively as in figure 1. The radius of the circle is $r = 6\,\mu m$

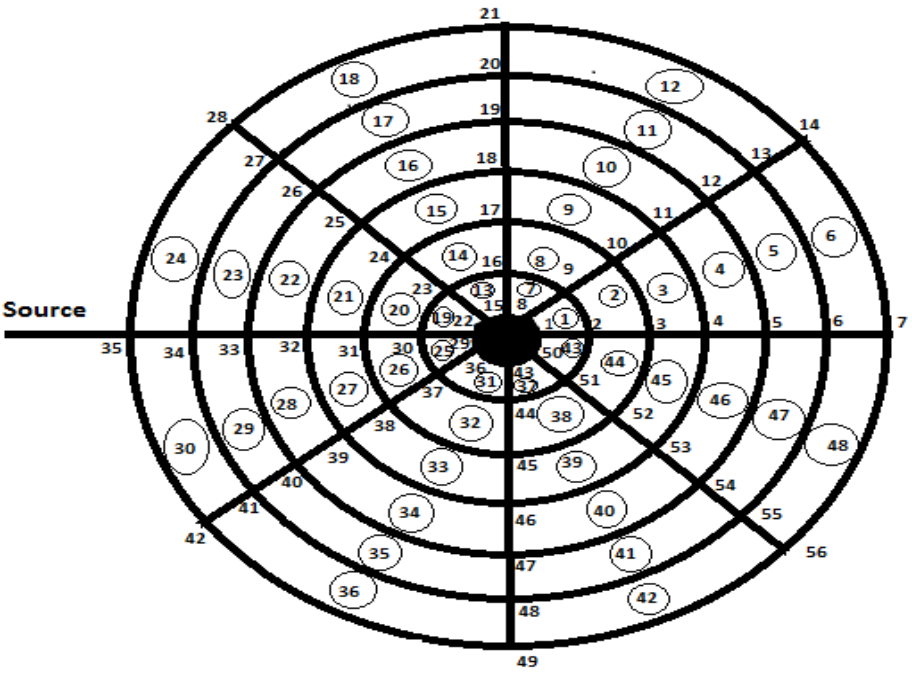

Figure 1. Discritization of circular Hepatocytes

The point source of calcium concentration is at $(r \to 6, \psi \to \pi)$ near the source. Taking the boundary condition as [5, 10, 11]:

$$\lim_{r \to 6, \psi \to \pi} \left(-2\pi r D_C \frac{d[C]}{dr} \right) = \sigma_C \tag{8}$$

Far from the source at the boundary it considers that the background concentration of calcium at infinity is $0.1\ \mu M$.

$$\lim_{r \to 6,\ \psi \to 2\pi} [C] = [C]_\infty \tag{9}$$

The element information of circular shape hepatocytes is described in table 1

Table 1. Element Information System

E	I_e	J_e	K_e	L_e
1	**1**	**2**	**8**	**9**
2	**2**	**3**	**9**	**10**
3	**3**	**4**	**10**	**11**
4	**4**	**5**	**11**	**12**
5	**5**	**6**	**12**	**13**
6	**6**	**7**	**13**	**14**
7	**8**	**9**	**15**	**16**

8	**9**	**10**	**16**	**17**
9	**10**	**11**	**17**	**18**
10	**11**	**12**	**18**	**19**
11	**12**	**13**	**19**	**20**
12	**13**	**14**	**20**	**21**
13	**15**	**16**	**22**	**23**
14	**16**	**17**	**23**	**24**
15	**17**	**18**	**24**	**25**
16	**18**	**19**	**25**	**26**
17	**19**	**20**	**26**	**27**
18	**20**	**21**	**27**	**28**
19	**22**	**23**	**29**	**30**
20	**23**	**24**	**30**	**31**
21	**24**	**25**	**31**	**32**
22	**25**	**26**	**32**	**33**
23	**26**	**27**	**33**	**34**
24	**27**	**28**	**34**	**35**
25	**29**	**30**	**36**	**37**
26	**30**	**31**	**37**	**38**
27	**31**	**32**	**38**	**39**
28	**32**	**33**	**39**	**40**
29	**33**	**34**	**40**	**41**
30	**34**	**35**	**41**	**42**
31	**36**	**37**	**43**	**44**
32	**37**	**38**	**44**	**45**
33	**38**	**39**	**45**	**46**
34	**39**	**40**	**46**	**47**

35	**40**	**41**	**47**	**48**
36	**41**	**42**	**48**	**49**
37	**43**	**44**	**50**	**51**
38	**44**	**45**	**51**	**52**
39	**45**	**46**	**52**	**53**
40	**46**	**47**	**53**	**54**
41	**47**	**48**	**54**	**55**
42	**48**	**49**	**55**	**56**
43	**50**	**51**	**1**	**2**
44	**51**	**52**	**2**	**3**
45	**52**	**53**	**3**	**4**
46	**53**	**54**	**4**	**5**
47	**54**	**55**	**5**	**6**
48	**55**	**56**	**6**	**7**

Equations (7) discretized in variational form

$$I^{(e)} = \frac{1}{2}\iint_A \left\{ r\left(\frac{d[c]^{(e)}}{dr}\right)^2 + \frac{1}{r}\left(\frac{d[c]^{(e)}}{d\psi}\right)^2 + \frac{1}{\lambda}\left([c]^{(e)2} - 2[c]^{(e)}\,[c]_\infty\right) r \right\} dA - \mu^{(e)} \int_{\psi_i}^{\psi_j} \left(\frac{\sigma}{2\pi D_C} [c]^{(e)}|_{r=6} \right) d\psi \tag{10}$$

where, e represents the number of elements $e = 1, 2, 3, ..., 48$. It is observed at the element $\mathbf{e} = 35$ that the value of $\left(\mu_{(e)} = 1\right)$ and the value $\left(\mu_{(e)} = 0\right)$ for the rest of all elements. Here, the bilinear shape function is considered as [8,12-14].

$$[c]^{(e)} = N_1^{(e)} + N_2^{(e)} r + N_3^{(e)} \psi + N_4^{(e)} r\psi \tag{11}$$

$$[c]^{(e)} = P^T N^{(e)} \tag{12}$$

where, $P^T = [1 \quad r \quad \psi \quad r\psi]$

and $(N^{(e)})^T = [N_1^{(e)} \quad N_2^{(e)} \quad N_3^{(e)} \quad N_4^{(e)}]$

From equation (11) & (12),

$$\overline{[C]^{(e)}} = P^{(e)} N^{(e)} \tag{13}$$

where, $\overline{[C]^{(e)}} = \begin{bmatrix} [C]_i \\ [C]_j \\ [C]_k \\ [C]_l \end{bmatrix}$ and

$$P^{(e)} = \begin{bmatrix} 1 & r_i & \psi_i & r_i\psi_i \\ 1 & r_j & \psi_j & r_j\psi_j \\ 1 & r_k & \psi_k & r_k\psi_k \\ 1 & r_l & \psi_l & r_l\psi_l \end{bmatrix}$$

We have from equation (11)

$$N^{(e)} = K^{(e)} \overline{[C]^{(e)}} \tag{14}$$

where, $K^{(e)} = P^{(e)-1}$

Putting the value of $N^{(e)}$ in equation (12),

$$[C]^{(e)} = P^T K^{(e)} \overline{[C]^{(e)}} \tag{15}$$

Taking integral $I^{(e)}$ is

$$I^{(e)} = I_k^{(e)} + I_m^{(e)} - I_s^{(e)} - I_z^{(e)} \tag{16}$$

where,

$$I_k^{(e)} = \frac{1}{2} \int_{\psi_i}^{\psi_k} \int_{r_i}^{r_j} \left[r \left(\frac{d[C]^{(e)}}{dr} \right)^2 + \frac{1}{r} \left(\frac{d[C]^{(e)}}{d\psi} \right)^2 \right] dr d\psi$$

$$I_m^{(e)} = \frac{1}{2} \int_{\psi_i}^{\psi_k} \int_{r_i}^{r_j} \left[\frac{1}{\lambda} [C]^{(e)2} r \right] dr d\psi$$

$$I_s^{(e)} = \int_{\psi_i}^{\psi_k} \int_{r_i}^{r_j} \left[\frac{1}{\lambda} [C]^{(e)} [C]_\infty r \right] dr d\psi$$

$$I_z^{(e)} = \mu^{(e)} \int_{\psi_i}^{\psi_j} \left(\frac{\sigma}{2\pi D_C} [C]^{(e)} \big|_{r=6} \right) d\psi$$

$$\frac{dI^{(e)}}{d\overline{[C]^{(e)}}} = \frac{dI_k^{(e)}}{d\overline{[C]^{(e)}}} + \frac{dI_m^{(e)}}{d\overline{[C]^{(e)}}} - \frac{dI_s^{(e)}}{d\overline{[C]^{(e)}}} - \frac{dI_z^{(e)}}{d\overline{[C]^{(e)}}} \tag{17}$$

On substituting values

$$\frac{dI}{d\overline{[C]}} = \sum_{e=1}^{M} \overline{G}^{(e)} \frac{dI^{(e)}}{d\overline{[C]^{(e)}}} \overline{G}^{(e)T} \tag{18}$$

where,

$$\overline{G}^{(e)} = \begin{bmatrix} 0 & 0 & 0 & 0 \\ . & . & . & . \\ 1 & 0 & 0 & 0 \\ 0 & 1 & 0 & 0 \\ 0 & 0 & 1 & 0 \\ 0 & 0 & 0 & 1 \\ . & . & . & . \\ 0 & 0 & 0 & 0 \end{bmatrix} \text{ and } \quad I = \sum_{e=1}^{48} I^{(e)} \tag{19}$$

Calcium concentration with respect to each nodal point for the maximum value of integral I is $[C]_i = (i = 1,2,3,.....48)$. This model provides the system of ODE, and is solved by the Gaussian Elimination Method [5, 8-11].

$$\left[\overline{X}\right]_{56\times 56}\left[\overline{[C]}\right]_{56\times 1} = \left[\overline{Y}\right]_{56\times 1} \tag{20}$$

Here, $\overline{[C]} = [C]_1[C]_2.....[C]_{56}$, $\overline{Y}$ is system vector and $\overline{X}$ are the system matrices, A computer program is used to analyze solution in MATLAB 2010b on Core(TM) i3 CPU 2328 with 4GB RAM @ 2.20 GHz processing speed.

3. Analysis of Results

The biophysical parameters are used to compute the results [4,6].

Table 2 Biophysical parameters

Biophysical Parameter	**Symbol**	**values**
Coefficient of diffusion	D_c	30 -150μ M^2 S^{-1}
Source amplitude	σ_C	1PA
Buffer association rate	K^+	0.1-0.5 μ M^{-1} S^{-1}
Buffer concentration	$[P]_\infty$	10 to100 μM
Background Ca^{2+} concentration	$[C]_\infty$	0.1 μM
Faraday's Constant	F	96500 C/M
Radius of cell	R	6 μm
Ca^{2+} Valence	Z	2

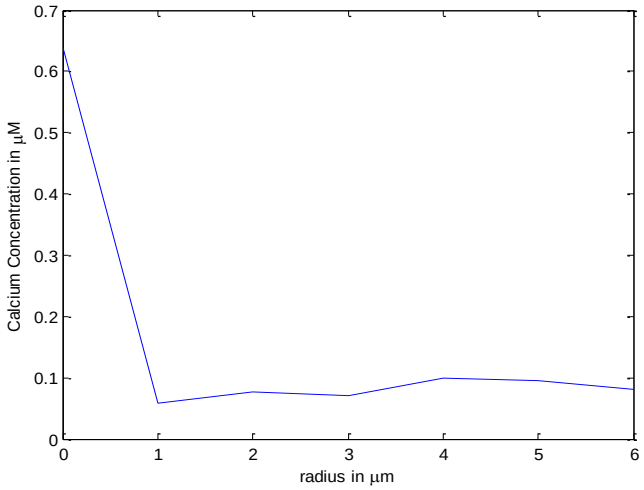

Figure 2. Graph between radial distribution and calcium concentrations in Hepatocytes

In figure 2, the calcium concentration goes down sharply between radius (r) 0-1 μM. After that it tends the background concentration 0.1μM. The free calcium enters into the hepatocytes cell and buffer that already exists near the plasma membranes, reacts with free calcium and create bound buffer. Thus, the effect of buffer plays a significant role. Here, we take the diffusion coefficients $D_c = 30\mu M^2 S^{-1}$.

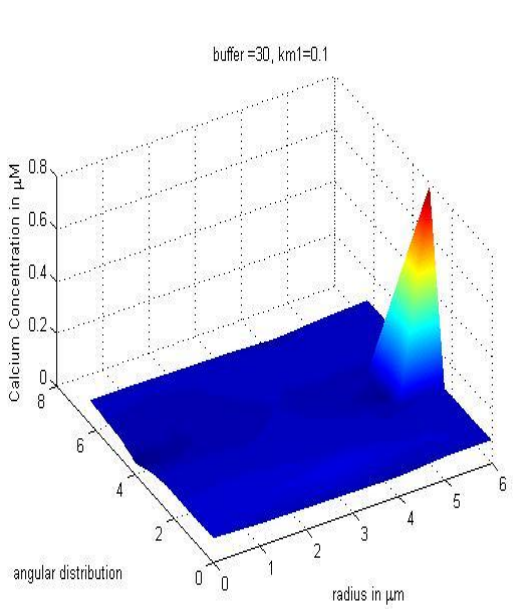

3 (a)

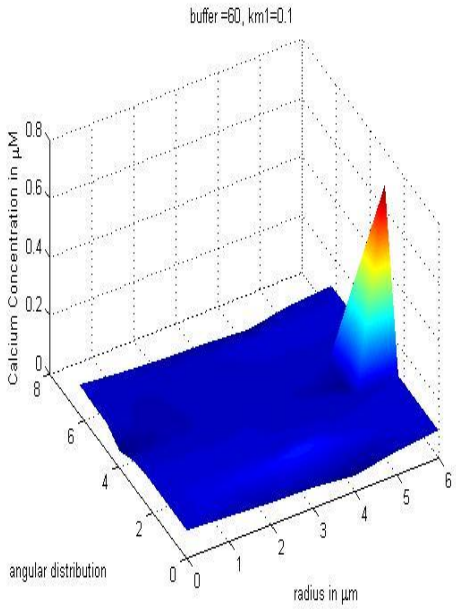

3 (b)

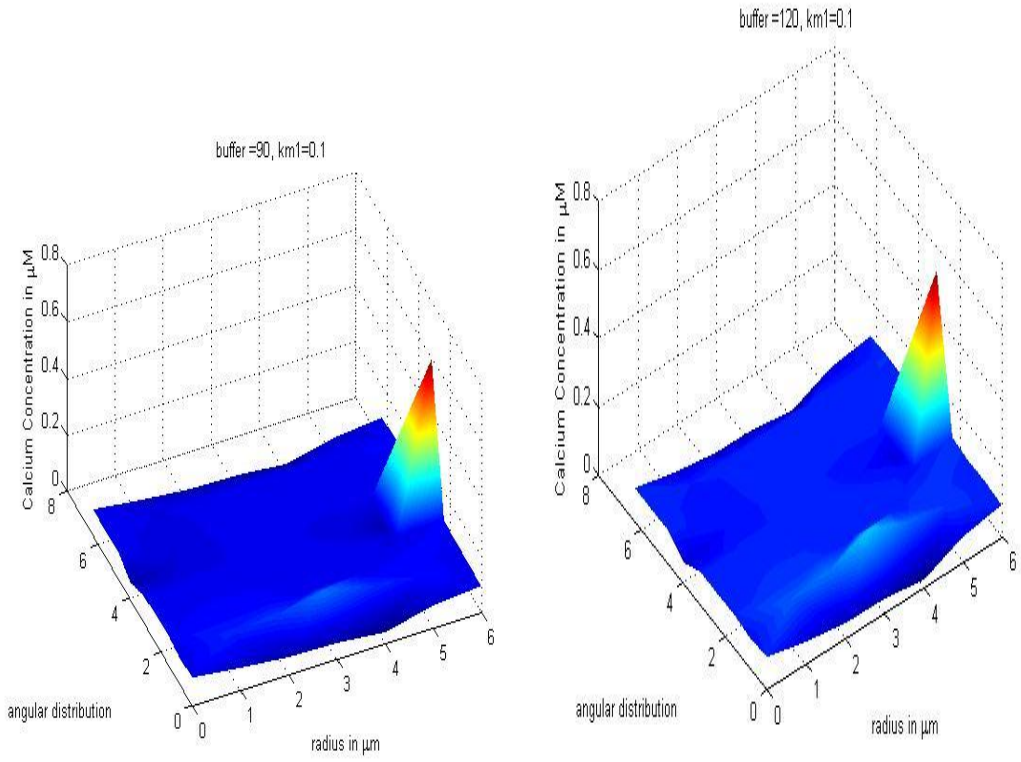

3 (c) **3 (d)**

Figure 3. Radial distribution of Ca^{2+}-concentration with different concentration of buffer.

In figure (3) radial and angular $Ca2^{+}$ distribution has been shown. The figure 3(a) showing protein (buffer) concentration is taken as 30 μM with higher affinity 0.1. It is seen that concentration of calcium is highest at the source ($r = 6$ and $\psi = \pi$). Concentration of Calcium decreases rapidly in both radial and angular as it moves gradually from the source and attends the concentration of background 0.1 μM . In figure 3(b) same amount of buffer (40 μM) is taken with lower affinity (0.1 μM). Concentration of calcium is higher at source in comparison to the figure 3(b). Far from the source it decreases. Cause of less affinity buffer reacts with less amount of free calcium ion as compared to the buffer 3(a). In figure 3(c) less amount of protein (buffer) takes the high affinity (0.5). It is observed that calcium profile is higher as compared to the figure 3(a). In both figures the affinity of the buffer is same but due to difference in amount of buffer less free calcium ion is bounded by buffer.

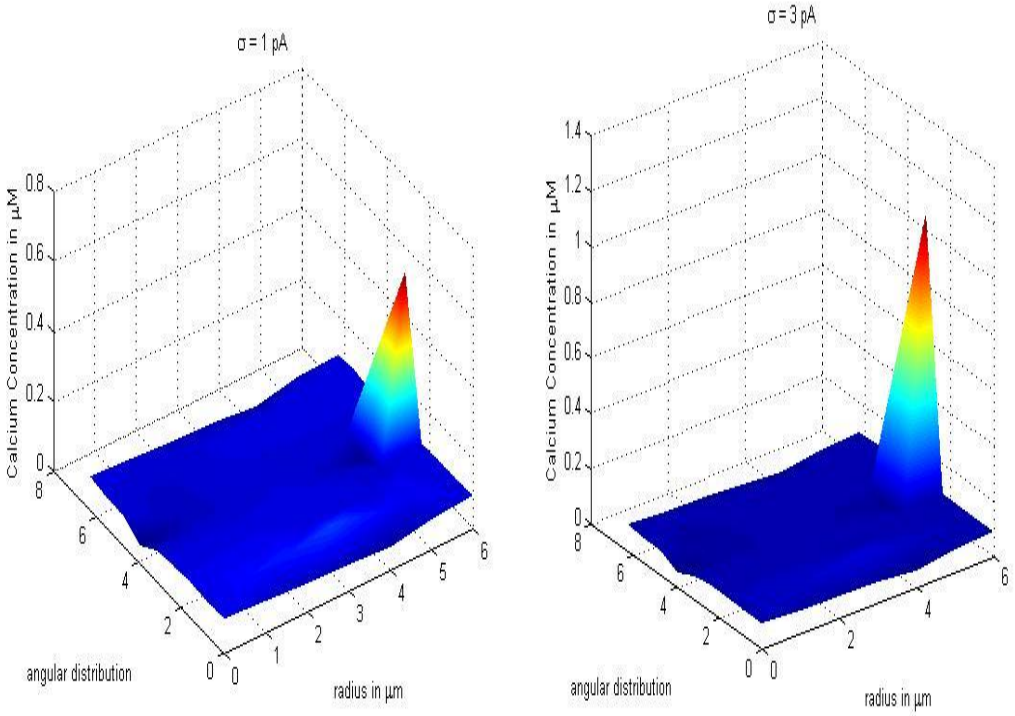

4(a) 4(b)

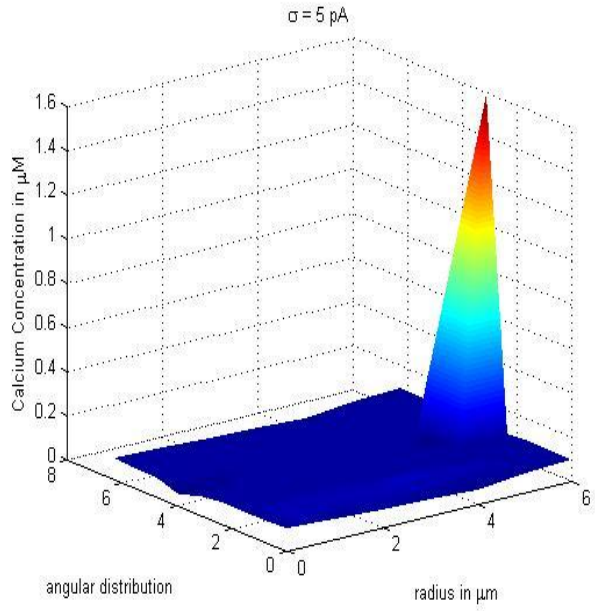

4(c)

Figure 4. Flux effect on calcium Concentration

In figure (4), the radial distribution on concentration of calcium or buffer for various values of flux is presented. It has been seen that concentration of calcium is on higher side for higher values of flux sigma (σ) = 3pA. Ca^{2+} profiles lie near the source and they converge to Ca^{2+} concentration is 0.1 μM after r=1.5 μm. It shows that the flux has significant effect on Ca^{2+} concentration near the source for constant value or buffer, comparing the curves for different values of σ_{Ca}, we observed that the rise in concentration of calcium is more for large values of

sigma (σ). This implies that the concentration of calcium near the source is with increase in influx σ_{Ca}.

4. Conclusion

This computational model gives us the interesting result regarding relationships among the various essential biophysical parameters as concentration of calcium, coefficients of diffusion, radius of hepatocytes, bound buffer etc. In the observation it is seen that the significant effect of concentration of calcium is more at point source regions in comparison to little away from the source. The finite element method is a powerful tool to deal such types of problems and provides quite accurate results of the problem. Here the circular elements give us better approximations to see the effect of calcium concentration in the cell.

References

[1] J. Wanger and J. Keizer, "Effect of Rapid Buffers on Ca^{2+} Diffusion & Ca^{2+} Oscillations", Biophysical Journal, vol. 67, **(1994)**, pp. 447- 456.

[2] M. H. Nathanson and S. F. Schlosser, "Calcium Signaling Mechanisms in Liver in Health and Disease" Prog. Liver Dis., no. 14, **(1996)**, pp. 1–27.

[3] M. Berridge, "Elementary and Global Aspects of Calcium Signaling" The Journal of Physiology, vol. 499, **(1997)**, pp. 291–306.

[4] S.Schuster, M. Marhl and T. Hoffer, "Modelling of Simple and Complex Calcium Oscillations from Single-Cell Responses to Intercellular Signaling" Euripean Journal of Biochemistry, vol. 269, no. (5), **(2002)**, pp.1333–1355.

[5] V. S. Rawat and N. Adlakha, "One Finite Elements Model to Study the Effect of Diffusion of Free Ca^{2+} in Hepatocytes", Procedia Computer Sciences, Elsevier. Vol. 57, **(2015),** pp. 923 – 928.

[6] M. Marhl, M. Gosak, M. Perc, J. C. Dixon and K. A. Green, "Spatio-Temporal Modeling Explains the Effect of Reduced Plasma Membrance Ca^{2+}Efflux on Intracellular Ca^{2+} Oscillation in Hepatocytes" Journal of Theoretical Boilogy, vol 252, no. (3), **(2008),** pp. 419-426.

[7] J. Crank, "The Mathematics of Diffusion". Oxford, U.K.: Clarendon Press, **(1975)**.

[8] C. P. Fall, "The Computational Cell Biology" Springer-Verlag New York, **(2002)**.

[9] E. Neher, "Concentration Profiles of Intracellular Ca^{2+} in the Presence of Diffusible Chelator". Experimental Brain Research, no.14, **(1986),** pp. 80-96.

[10] G. D. Smith, "Modeling Intracellular Calcium Diffusion, Dynamics and Domains" no 10, **(2004),** pp. 339-371.

[11] B. K. Jha, N. Adlakha and N. M. Mehta, "Two-Dimensional Finite Element Model to Study Calcium Distribution in Astrocytes in Presence of VGCC and Excess Buffer"

International Journal of Modeling, Simulation and Scientific Computing, vol. 4, no (2), **(2013),** pp. 5**.**

[12] Chander, S., Baishya, S., Sinha, S. K., Kumar, S., Singh, P. K., Baral, K., ... & Jit, S. (2019). Two-dimensional analytical modeling for electrical characteristics of Ge/Si SOI-tunnel FinFETs. *Superlattices and Microstructures*, *131*, 30-39.

[13] S. S. Rao, "Finite Element Method in Engineering" Elsevier Science and Technology, **(2004).**

[14] E. M. Gracheva, R. Toral, D. J. Gunton, "Stochastic Effects in Intercellular Calcium Spiking in Hepatocytes", Journal of Theoretical Biology, vol. 212, **(2001)**, pp. 111-125.

Authors

Vijendra Singh Rawat has received his M. Phil degree in Mathematics in 2010. He is having more than 10 years of experience in teaching. His area of interests are Mathematical modeling and computational biology. He is presently working as Assistant Professor in Department of Mathematics, Teerthanker Mahaveer University, Moradabad, U. P., India.

Rinku Mathur has received his PhD degree in Mathematics in 2014. He is having 8 years of experience in teaching. His area of interests are Mathematical modeling, evolutionary biology and computational biology. He is presently working as Assistant Professor in Department of Mathematics, Lovely Professional University, Phagwara, Punjab, India.